Available online at www.sciencedirect.com
SCIENCE DIRECT®
PERGAMON
Polyhedron 22 (2003) 3129–3135
POLYHEDRON
www.elsevier.com/locate/poly

$Cd(NH_2CSNHNHCSNH_2)Cl_2$: a new single-source precursor for the preparation of CdS nanoparticles

P. Sreekumari Nair [a,1], Thottackad Radhakrishnan [a,2,3], Neerish Revaprasadu [a], Gabriel A. Kolawole [a], Paul O'Brien [b,*]

[a] *Department of Chemistry, University of Zululand, Private Bag X 1001, KwaDlangezwa 3886, South Africa*
[b] *The Manchester Materials Science Centre and Department of Chemistry, Manchester University, Oxford Road, Manchester M13 9PL, UK*

Received 11 April 2003; accepted 7 July 2003

Abstract

The complex of cadmium with dithiobiurea, $[Cd(NH_2CSNHNHCSNH_2)Cl_2]$, has been used as a precursor for the synthesis of CdS nanoparticles. The precursor was decomposed in tri-*n*-octylphosphine oxide to give CdS nanoparticles that show quantum confinement effects with characteristic close to band edge luminescence. The broad diffraction in the XRD pattern and diffused diffraction rings of the SAED pattern are typical of nanometer-sized particles. The particle morphology was found to depend on the temperature of injection of the precursor. Transmission electron microscopy shows irregular non-spherical particles prepared by injection at 150 °C, whilst with injection at 240 °C the particles are formed as spherical aggregates of relatively uniform size (50 nm).

Keywords: Cadmium sulfide; Nanocrystallites; Single-source precursor method

1. Introduction

Nanometer-sized semiconductor crystallites exhibit properties different from those of the bulk and are a new class of materials which hold considerable promise in numerous applications in both electronics and photonics [1–4]. The uniqueness of these particles lies in their size dependent electronic and optical properties arising from the quantum size effects and the large number of unsaturated surface atoms. Much current work has been focused on harnessing these properties in the fabrication of electronic devices such as light emitting diodes (LEDs) or quantum dot lasers [5]. In such applications, the nanoparticles should have uniform size, shape and crystallinity. Various reports have appeared on different types of semiconductor nanocrystals, including colloidal particles [6–9] and samples embedded in glass matrices [10] or zeolitic cages [11,12]. In order to prevent agglomeration of particles the surface atoms are passivated by long-chain organic surfactants, or by capping agents including, TOPO, pyridine, alkyl amines, or thiols [13]. Another type of nanoparticles is the core–shell structures in which a layer of a second semiconductor is deposited onto a semiconductor nanocrystallite which serves as the core of the core–shell structure [14]. Such structures include compositions such as CdS on ZnS [15], CdSe on ZnS [16], CdSe on ZnSe [17], and HgS on ZnS [18]. This type of work has been further extended to the synthesis of a quantum dot quantum well (QDQW) in which a three layered structure consisting of, for example, a CdS nanocrystallite forms an inner core and a layer of HgS covering this core, followed by CdS as the outer shell [19]. Brus [21], Henglein [20], and Weller [11] have carried out pioneering work in the synthesis and photophysical properties of semiconductor nanocrystallites [11,20,21].

One common route for the synthesis of semiconductor nanoparticles is a controlled precipitation reaction

* Corresponding author. Tel.: +44-161-275-4652; fax: +44-161-275-4616.
E-mail address: paul.obrien@man.ac.uk (P. O'Brien).
[1] Present address: Department of Chemistry (Lash Miller Chemical Laboratory), 80, St. George Street, University of Toronto, Ontario, Canada, M5S 346.
[2] Present address: Department of Chemistry, University of Toronto at Mississanga, 3359, Mississanga Road, Ontario, Canada, L5L 1C6.
[3] Permanent address: Department of Chemistry, University of Kerala, Trivandrum, India 695581.

0277-5387/$ - see front matter © 2003 Published by Elsevier Ltd.
doi:10.1016/S0277-5387(03)00458-3

giving dilute suspension of colloidal particles [22]. Murray et al. [23] have synthesized CdS nanoparticles by the pyrolysis of organometallic reagents on injection into a coordinating solvent, TOPO. The nanocrystallites prepared by this method have greater crystallinity than those obtained by colloidal methods. We have modified this method by the use of simple cadmium salts [24], a method that has been emulated by others. The use of highly hazardous and volatile compounds such as dimethylcadmium, and noxious compounds such as H_2S has led to the development of safer and more environment-friendly routes for the synthesis of semiconductor nanocrystallites. We have earlier reported the use of dithiocarbamates and selenocarbamates of divalent metals as single-source precursors for the deposition of high quality monodispersed nanoparticles [25]. The particles were prepared by the thermolysis of the precursor in coordinating solvents like TOPO or 4-ethylpyridine. The as prepared particles were further processed by size-selective precipitation techniques to give particles of very narrow size and size distribution. However, the limitation imposed on such methods includes the use of toxic compounds such as CE_2 (E = S or Se) for the synthesis of the precursor compounds. Here, we report the synthesis of TOPO capped CdS nanoparticles using cadmium complex of dithiobiurea as a single-source precursor. The synthesis of the precursor complex from the commercially available compounds involves a simple synthetic procedure.

2. Experimental

Methanol, toluene, cadmium chloride, and dithiobiurea used in the synthesis were analytical grade reagents. Tri-*n*-octylphosphine (TOP) (Aldrich) was used as supplied. TOPO was purified by the method described in the literature [26]. All other chemicals were used as provided by the manufacturer.

3. Instrumentation

3.1. UV–Vis, IR, spectroscopy

A Perkin–Elmer Lambda 20 UV–Vis spectrophotometer was used to carry out optical measurements. Samples were placed in quartz cuvettes (1 cm path length). Infrared spectra were taken on Perkin–Elmer Paragon 1000 FT-IR spectrometer, as KBr pellets.

3.2. Thermogravimetric analysis

Thermogravimetric analysis of the precursor was carried out with a Perkin–Elmer Pyris 6 TGA in nitrogen atmosphere at a heating rate of 10 °C/min.

3.3. Photoluminescence spectroscopy

A Jobinyvon-spex-Fluorolog-3-Spectrofluorimeter with xenon lamp was used to measure the photoluminescence of the nanocrystallites. The samples were placed in quartz cuvettes (1 cm path length).

3.4. X-ray diffraction

The wide-angle X-ray diffraction (XRD) was recorded using Philips X'Pert Materials Research Diffractometer. Measurements were taken using a glancing angle incidence detector at an angle of 3° for 2θ values over 5–60° in steps of 0.04° with a count time of 2 s.

3.5. Electron microscopy

A JEOL JEM-1200EXII transmission electron microscope using JEOL EM-ACD10 anticontamination device was used for the conventional transmission electron microscopy (TEM) measurements. The operating voltage was 80–100 kV. The EDAX plots were obtained using the LINK QX2000 Energy Dispersive Analysis System operating at 25 kV at a tilt angle of 30°. The samples were deposited onto carbon-filmed grids using a fine pipette, air-dried, and immediately examined by the microscope.

3.6. Preparation of $Cd(NH_2CSNHNHCSNH_2)Cl_2$

$CdCl_2 \cdot H_2O$ 0.201 g (0.001 mol) was dissolved in 50 mL water. This solution was added to a hot solution of dithiobiurea 0.15 g (0.001 mol) in 50 mL water. A solid product was formed which was digested over a water bath for 30 min. It was then cooled, filtered washed with water, and dried at room temperature. Yield 0.21 g (63%) C, H, N, S analyses %, experimental (calculated), $CdC_2H_6N_4S_2Cl_2$: C, 7.3 (7.2); H, 1.8 (1.80); N, 16.7 (16.8); S, 19.3 (19.2).

3.7. Synthesis of CdS nanoparticles

The precursor, $Cd(NH_2CSNHNHCSNH_2)Cl_2$ (1.1 g) was dispersed in 10 mL TOP. This mixture was then injected into TOPO (20 g) at 150 °C. The temperature of the reaction mixture was found to drop by 15–20 °C. The solution appears to be turbid and gray. The temperature was then slowly raised to 250 °C and the color of the solution turned yellow. Heating was continued for another 3 h at 250 °C. The solution was then cooled to 70 °C and excess methanol was added. The yellow solid formed was separated by centrifugation and re-dissolved in toluene for further analysis. Another set of samples was prepared by the same set of experimental conditions except that the injection temperature was 240 °C.

4. Results and discussion

The results of the thermogravimetric analysis of the precursor are given in Fig. 1. The decomposition starts at 230 °C and is complete by 800 °C. The TGA curve serves as a guide in deciding the injection temperature for the precursor into TOPO. We decided to prepare two sets of samples one from injecting the precursor at 150 °C, below the decomposition temperature of the precursor and a second with injection at 240 °C, above the decomposition temperature of the precursor. This approach was adopted to monitor the effects on the size and morphology of the resultant particles. When the precursor was injected into TOPO at 150 °C, there was no sudden decomposition as evidenced by the absence of any immediate yellow coloration of the solution. The sudden drop in temperature on injecting a cold dispersion of the precursor in TOP into hot TOPO also will have little or no influence on the nucleation or growth of crystallites as the injection temperature is well below the decomposition temperature of the precursor. As the temperature of the solution was increased decomposition of the precursor occurred with the appearance of yellow color in the reaction mixture. In this slow decomposition process, the nucleation begins and as temperature is further increased there are two competing processes occurring, i.e., the nucleation and the growth of nuclei already formed.

In the second case, when the injection of the precursor was at 240 °C, i.e., above the decomposition temperature of the precursor, there should be sudden decomposition of the precursor leading to rapid nucleation. However, the sudden drop in temperature probably prevents further nucleation and as temperature is increased controlled growth and annealing of the crystallites occur [23].

4.1. Optical properties of CdS nanoparticles

The optical absorption spectrum of a toluene solution of the CdS nanoparticles obtained by the thermal decomposition of the precursor complex, $Cd(NH_2CSNHNHCSNH_2)Cl_2$, injected into TOPO at 150 °C is shown in Fig. 2. The absorption edge shows a blue shift with respect to bulk CdS (515 nm, 2.4 eV) [20–25]. This absorption edge of CdS sample obtained by injecting the precursor into TOPO at 150 °C, as calcu-

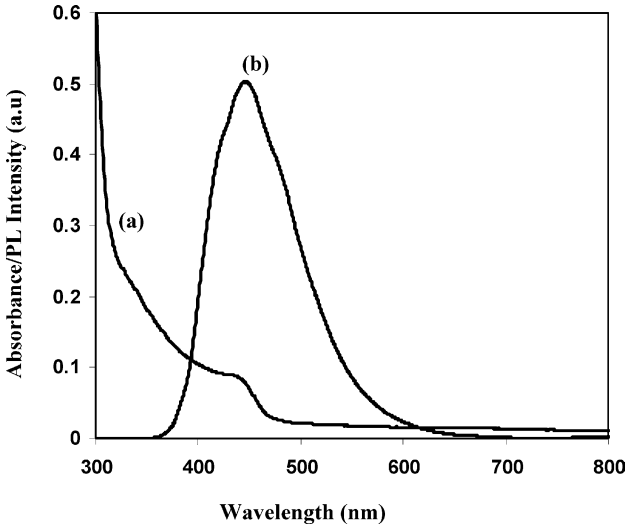

Fig. 2. (a) Optical absorption and (b) photoluminescence spectra of TOPO capped CdS nanoparticles by synthesized at 150 °C.

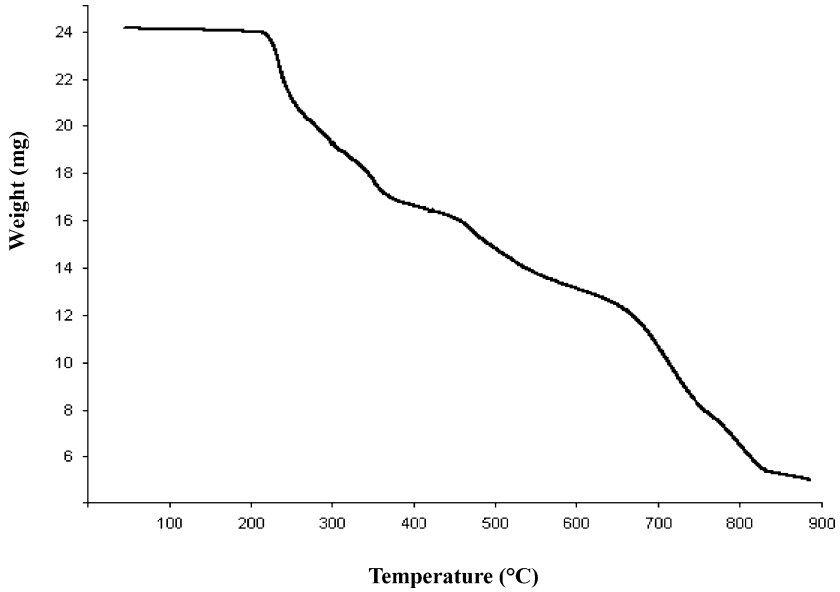

Fig. 1. TGA curve for $Cd(NS_2CSNH_2)_2Cl_2$ carried out under nitrogen atmosphere, at a heating rate of 10 °C/min.

lated by the direct band gap method [27], is 478 nm (2.59 eV) (Fig. 2), showing a blue shift of 37 nm in relation to that of the bulk material. The UV–Vis spectrum also shows a sharp excitonic feature at 450 nm which could be indicative of a highly monodispersed sample [23]. The calculation of the CdS particle diameter using the effective mass approximation (EMA) model [28] gives a value of 5.4 nm. The absorption spectra of CdS nanoparticles obtained by injecting the precursor at 240 °C is shown in Fig. 3. The sharp excitonic feature that is visible in the spectrum of CdS nanoparticles obtained at a lower injection temperature is less evident. The band edge calculated at 485 nm (2.55 eV) shows a blue shift in relation to the bulk material. The shape of the spectrum is indicative of a slightly less monodisperse sample than the one obtained by the injection of the precursor at 150 °C.

The photoluminescence spectrum of the CdS sample obtained by injecting the precursor into TOPO at 150 °C shows an emission maximum at 450 nm ($\lambda_{exc} = 380$ nm) (Fig. 2). The CdS sample obtained after injection at 240 °C shows an emission maximum at 495 nm ($\lambda_{exc} = 380$ nm) (Fig. 3). Previous reports suggest that the emission arises from the recombination of an electron trapped in a sulfur vacancy with a hole in the valence band of CdS [29]. The electrons generated by the absorption of photons can be trapped into sulfur vacancies through a radiation-less decay followed by the recombination with holes in the valence band. It is argued that creation of sulfur vacancies in CdS nanocrystallites prepared by reacting Cd^{2+} with a S^{2-} source is due to the formation of non-stoichiometric CdS consequent to the slow generation of S^{2-} ions in the reaction medium which is insufficient to form a stoichiometric CdS crystallite [30]. Studies on CdS and CdSe nanoparticles also showed emission spectrum due to the vacancies of the chalcogenide ions. These crystallites were derived from single-source precursors such as bis(hexylmethyldithio-/diselenocarbamato)cadmium(II) [31], methyldiethyldiselenocarbamato cadmium(II) [32], cadmium ethylxanthate [33], and cadmium(II) complex of thiosemicarbazide [34] which have Cd:chalcogen atom ratio that varies from 1:4 to 1:2. Hence it should be concluded that creation of chalcogenide ion vacancies is extraneous to the effect of its availability in the reaction medium, rather it is governed by the intrinsic growth mechanism of the crystallites under the reaction conditions.

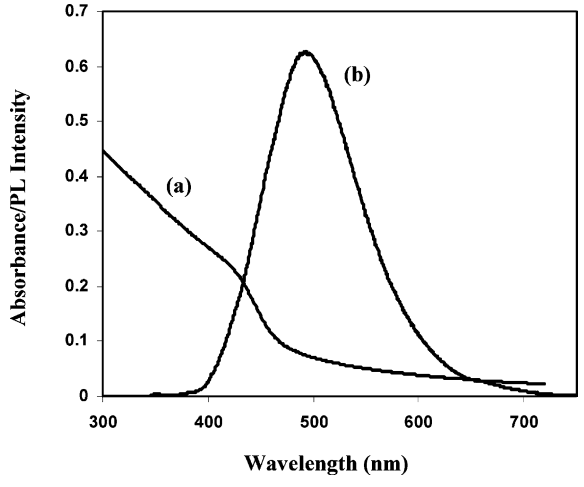

Fig. 3. (a) Optical absorption and (b) photoluminescence spectra of TOPO capped CdS nanoparticles synthesized at 240 °C.

4.2. Structural studies of CdS nanoparticles

TEM images of the nanoparticles are given in Fig. 4. The optical properties of the particles obtained by injecting the precursor into TOPO at 150 and 240 °C indicate that the primary particles in both the cases are in the same size range. The TEM images show that the particles which were obtained by injecting the precursor at 150 °C had an irregular, slightly non-spherical shape with an average particle size of 5.5 nm (±6%). However, the TEM images of the particles obtained from the injection of the precursor at 240 °C are seen as spherical aggregates of about 50 nm. The particles are in the same size range as those obtained at 150 °C, however the determination of their size distribution is difficult as a result of the aggregation. The mechanism of formation of such aggregates has been studied in detail and the agglomeration time required to reduce the concentration of the crystallites by half, $t_{1/2}$, has been calculated [35]. The cardinal steps involved in the formation of crystallites from solutions are the nucleation and growth, but the rapid aggregation process prevents the individual nanoparticles growing to larger particles [30].

The EDAX spectrum gives strong peaks for cadmium, sulfur, and phosphorous. The phosphorous peak arises from the capping agent TOPO. The presence of TOPO is further confirmed by IR spectroscopy. The CdS particle shows a band around 1450 cm^{-1} which can be assigned to ν_{sym}, P=O. Similar shifts in IR frequencies of TOPO capped nanoparticles are reported in the literature [36]. Bulk CdS usually exists in the hexagonal phase whereas, the nanoparticles can exist as either the cubic or the hexagonal phase [37]. Even though there are many reports of CdS nanoparticles existing in hexagonal phase, the existence of a mixture of cubic and hexagonal phase with the predominance of one over the other is also a possibility, as reported by Bawendi et al. [38]. The wide-angle X-ray diffraction pattern of the nanocrystallites obtained at 150 °C is shown in Fig. 5(a). The XRD peaks are broadened compared to those of the bulk CdS indicating that the particles are in the nanosize regime. However, the (1 1 0), (1 0 3), and (1 1 2) planes of wurtzite CdS are clearly distinguishable in the diffraction pattern. The SAED pattern (Fig. 5(b)) consists of broad diffuse rings, which are indicative of the small size

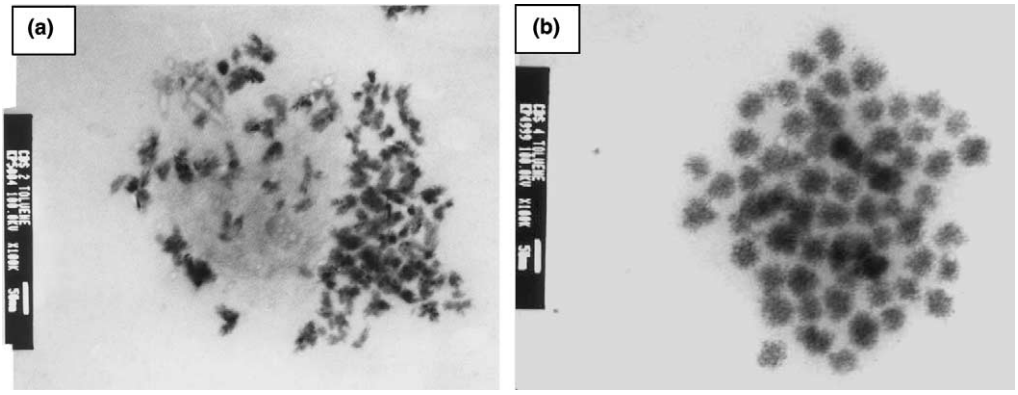

Fig. 4. TEM image of CdS nanoparticles synthesized at (a) 150 °C and (b) 240 °C.

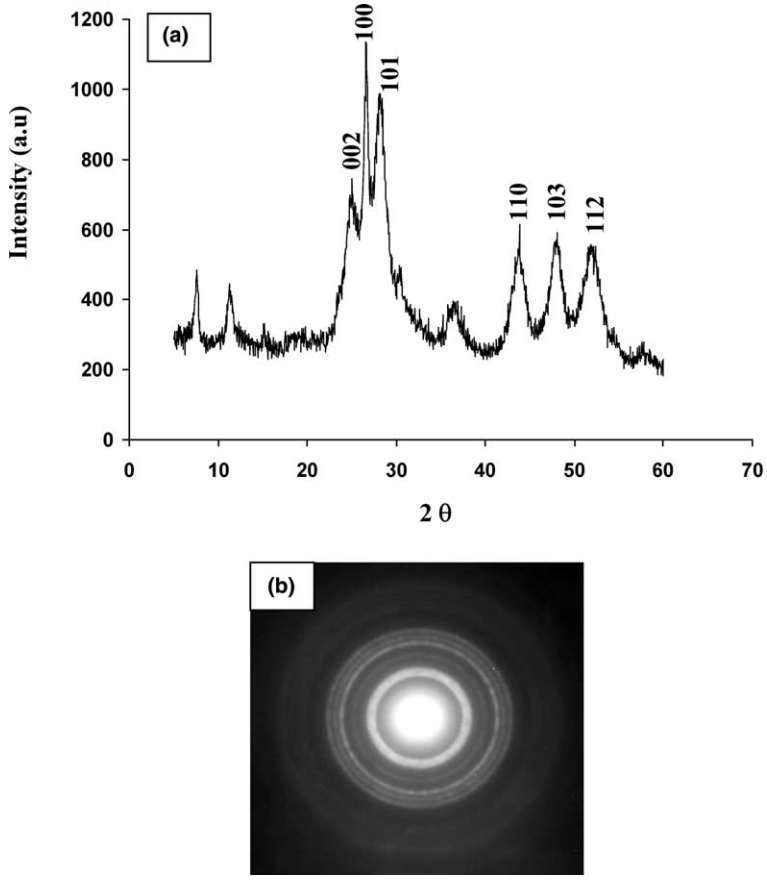

Fig. 5. (a) X-ray diffraction pattern (indexed to hexagonal phase) and (b) selected area diffraction pattern (SAED) of CdS nanoparticles synthesized at 150 °C.

of the particles. The diffraction rings can be indexed to the (1 0 0), (1 0 2), (1 0 3), and (1 1 2) planes confirming the wurtzite phase. The mean crystallite diameter, d, can be calculated by the Scherrer formula [39]

$$d = 0.94\ \lambda/B\mathrm{Cos}\,\theta,$$

where λ is the X-ray wavelength, B is the full width at half maximum of the diffraction peak on the 2θ scale. The crystallite sizes were determined using the (1 0 3) reflection at 47.902° (2θ) and the calculated value is found to be 5.1 nm which is in good agreement with the size obtained in TEM measurements. The XRD pattern of the CdS nanoparticles obtained at an injection temperature of 240 °C also confirms a wurtzite structure of CdS (Fig. 6(a)). However, the (0 0 2), (1 0 0), and (1 0 1) planes that are clearly visible in the 150 °C sample appear broadened as a single peak. The (1 1 0), (1 0 3), and (1 1 2) planes also appear slightly broader. The broader

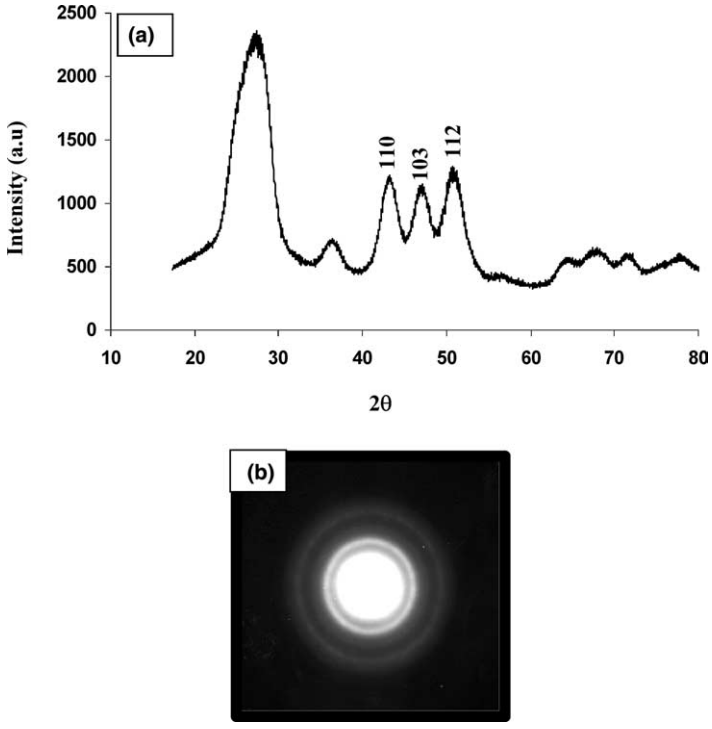

Fig. 6. (a) X-ray diffraction pattern (indexed to hexagonal phase) and (b) selected area diffraction pattern (SAED) of CdS nanoparticles synthesized at 2400 °C.

peaks of the 150 °C are indicative of a smaller particle size as confirmed by the Scherrer equation which estimates the particle diameter size to be 4.2 nm.

5. Conclusions

In the present study, we have synthesized a new complex by reacting cadmium chloride with dithiobiurea with a view to its use as a single-source precursor for the preparation of CdS nanoparticles. TOPO capped CdS nanoparticles were prepared by the thermolysis of the new precursor. The nanocrystallite has wurtzite structure and shows quantum size effects, owing to which the band edge is shifted to lower wavelength as measured by the optical absorption spectra. The particle morphology was found to be controlled by the injection temperature of the precursor into the thermolyzing solvent. A lower temperature favored the formation of particles of irregular morphology, while at higher temperature nearly spherical aggregates of the nanoparticles are obtained.

Acknowledgements

We thank the Royal Society and the National Research Foundation (SA) for financial support. We also thank Judith Shackleton (Manchester Materials Science Centre) for the XRD and Keith Pell (QMW) for the TEM measurements.

References

[1] V.I. Klimov, A.A. Mikhailovski, S. Xu, A. Malko, J.A. Hollingsworth, A.A. Leatherdale, H.J. Eisler, M.G. Bawendi, Science 290 (2000) 314.
[2] M. Nirmal, L. Brus, Acc. Chem. Res. 32 (1999) 407.
[3] A.P. Alivisatos, J. Phys. Chem. 100 (13) (1996) 226.
[4] Z. Tang, N.A. Kotov, M. Giersig, Science 297 (2002) 237.
[5] B. Levy, J. Electroceram. 1,3 (1997) 239.
[6] W.W. Yu, X. Peng, Angew. Chem. Int. Ed. 41 (2002) 2368.
[7] J. Hambrock, A. Birkner, R.A. Fischer, J. Mater. Chem. 11 (2001) 3197.
[8] L.S. Li, J. Hu, W. Wang, A.P. Alivisatos, J. Am. Chem. Soc. 124 (2002) 7136.
[9] U.K. Gautam, M. Rajamathi, F. Meldrum, P. Morgan, R. Seshadri, Chem. Commun. (2001) 629.
[10] H. Shinojima, J. Yumoto, N. Uesugi, S. Omi, Y. Asahara, Appl. Phys. Lett. 55 (1989) 1519.
[11] H. Weller, Adv. Mater. 5 (1993) 88.
[12] H. Weller, Angew. Chem., Int. Ed. Engl. 32 (1993) 41.
[13] T. Trindade, P. O'Brien, N.L. Pickett, Chem. Mater. 13 (2001) 3843.
[14] N. Revaprasadu, M.A. Malik, P. O'Brien, G. Wakefield, Chem. Commun. (1999) 1573.
[15] H.C. Youn, S. Barl, J.H. Fendler, J. Phys. Chem. 92 (1988) 6320.
[16] A.R. Kortan, R. Hull, R.L. Opila, M.G. Bawendi, M.L. Steigerwald, P.J. Carroll, L.E. Brus, J. Am. Chem. Soc. 112 (1990) 1327.
[17] C.F. Hoener, K.A. Allan, A.J. Bard, A. Campion, M.A. Fox, T.E. Mallouk, S.E. Webber, J.M. White, J. Phys. Chem. 96 (1992) 3812.

[18] A. Eychmuller, A. Hasselbarth, H. Weller, J. Lumin. 53 (1992) 113.
[19] X. Peng, M.C. Schlamp, A.V. Kadavanich, A.P. Alivisatos, J. Am. Chem. Soc. 119 (1997) 7019.
[20] A. Henglein, Chem. Rev. 89 (1989) 1861.
[21] L.E. Brus, J. Phys. Chem. 98 (1994) 3575.
[22] H. Fendler, Adv. Mater. 7 (1995) 607.
[23] C.B. Murray, D.B. Norris, M.G. Bawendi, J. Am. Chem. Soc. 115 (1993) 8706.
[24] M. Lazell, P. O'Brien, J. Mater. Chem. 9 (1999) 1381.
[25] (a) T. Trindade, P. O'Brien, X. Zhang, M. Motevalli, J. Mater. Chem. 6 (1997) 1011;
(b) B. Ludolph, M.A. Malik, P. O'Brien, N. Revaprasadu, Chem. Commun. (1998) 1849;
(c) M.A. Malik, N. Revaprasadu, P. O'Brien, Chem. Mater. 13 (2001).
[26] R.A. Zingaro, J.C. White, J. Inorg. Nucl. Chem. 12 (1960) 315.
[27] J.L. Pankove, Optical Processes in Semiconductors, Dover Publications, New York, 1970.
[28] L.E. Brus, J. Phys. Chem. 90 (1986) 2555.
[29] N. Chestnoy, T.D. Harris, R. Hull, L.E. Brus, J. Phys. Chem. 90 (1986) 3393.
[30] G.Q. Xu, B. Liu, S.J. Xu, C.H. Chew, S.J. Chua, L.M. Gana, J. Phys. Chem. (2000) 829.
[31] M.A. Malik, N. Revaprasadu, P. O'Brien, Chem. Mater. 13 (2001) 913.
[32] T. Trindade, P. O'Brien, Adv. Mater. 8 (1996) 161.
[33] P. Sreekumari Nair, T. Radhakrishnan, N. Revaprasadu, G.A. Kolawole, P. O'Brien, J. Mater. Chem. 12 (2002) 2722.
[34] P. Sreekumari Nair, T. Radhakrishnan, N. Revaprasadu, G.A. Kolawole, P. O'Brien, Chem. Commun. (2002) 564.
[35] A. Celikkaya, M. Akine, J. Am. Ceram. Soc. (1990) 73245.
[36] J.E.B. Katari, V.L. Colvin, A.P. Alivisatos, J. Chem. Phys. 98 (1994) 4109.
[37] R.J. Bandaranayake, G.W. Wen, J.Y. Lin, H.X. Jiang, C.M. Sorensen, Appl. Phys. Lett. 67 (1995) 83.
[38] M.G. Bawendi, A.R. Kortan, M.L. Steigerwald, L.E. Brus, J. Chem. Phys. 91 (1989) 7282.
[39] B. Cullity, Elements of X-ray Diffraction, second ed., Addison-Wesley, Reading, MA, 1978.